First-Principles Determinations and Investigations of the Electronic Absorption and Third-Order Polarizability Spectra of Electron Donor−Acceptor Chromophores Tetraalkylammonium Halide/Carbon Tetrabromide†

Juan Shen, Wen-Dan Cheng,* Dong-Sheng Wu, Shu-Ping Huang, Hui Hu, and Zhi Xie

State Key Laboratory of Structural Chemistry, Fujian Institute of Research on the Structure of Matter, the Chinese Academy of Sciences, Fuzhou, Fujian 350002, People's Republic of China

Received: April 5, 2007; In Final Form: June 19, 2007

Calculations on donor−acceptor molecular pairs of tetraalkylammonium halide/carbon tetrabromide complexes are provided to investigate structure/property-related linear and nonlinear optical properties by using the time-dependent density functional theory technique coupled with the sum-over-states method. The calculated energies of the first allowed electronic transition decrease, and the nonresonant third-order polarizabilities at the THG, EFISHG, and DFWM optical processes increase progressively from [DBU−H^+Br^-·CBr_4] to [NPr_4Br·CBr_4] to [NMe_4Br·CBr_4]. The obtained electronic absorption spectra show a progressive red shift with increasing donor strength from Cl to I for [NR_4h·CBr_4] (h = Cl, Br, and I). The charge transfers from the halogen donor to the carbon tetrabromide acceptor make significant contributions to the electronic absorption spectra in the low-energy zone and the third-order polarizabilities in the nonresonant frequency region. The counterion indirectly affects the electronic absorption and third-order polarizability spectra through the interactions between the donor and acceptor.

1. Introduction

Materials with excellent nonlinear optical (NLO) properties are required in various fields of photonic device applications such as optical data storage, optical information processing, harmonic generators, optical switching, optical communication, and optical limiting.[1−6] These applications require materials with sufficiently large and fast third-order NLO responses.[7,8] Furthermore, the third-order NLO response is a basic means for light controlling with light in all optics, such as optical bistability and phase conjugation.[9]

Molecules exhibiting large third-order nonlinear polarizabilities are indispensable for understanding the all-optical switching, modulating, and optical limiting of laser pulses and holographic memory devices in modern optical technology.[10] During the past two decades, a great deal of basic and applied research on NLO materials has mainly focused on conjugated organic molecules and polymers; inorganic, organic, organometallic, and metal−organic polymers; and cluster and coordination compounds.[8,10−12] Recent years have witnessed an increased interest in the class of NLO chromophores constituted by donor−acceptor systems forming donor−π-donor (D−π-D), acceptor−π-acceptor (A−π-A), donor−acceptor−donor (D−A−D), and acceptor−donor−acceptor (A−D−A) structures.[13−16] Several conjugated organic molecules having strong donor−acceptor intermolecular interactions have been investigated, and they exhibit large third-order nonlinear optical properties. Moreover, fine-tuning of the NLO properties of compounds can be achieved by rational modification of the chemical structure. To enhance the application viability of NLO materials, current research should aim to understand the fundamental relationship between the optical response and the molecular structure. Quantum-chemical calculations have made important contributions to understanding the electronic polarization underlying molecular NLO processes and determining structure/property relationships and thus provided clues to the design of molecular complexes with large nonlinear optical susceptibilities.[8,9,14−17] Strong charge-transfer complexes of CBr_4 as a superior electron acceptor have been found, and the charge-transfer interactions in these complexes have been revealed in several studies.[18,19] Donor−acceptor-substituted tetraalkylammonium halide/carbon tetrabromide complexes form a series of diamondoid networks whose nonlinear optical responses are expected to be extensive.[19] Kochi et al.[19] investigated the unusual strength and directionality as well as the large electronic couplings between the halide donor and CBr_4 acceptor experimentally and pointed out that the charge-transfer nature of CBr_4−halide complexes represents a factor that is potentially favorable for high second-order hyperpolarizability. In earlier work in our group, we discussed the electronic origin of the nonresonant enhancement of second-order nonlinear optical responses in these complexes of noncentrosymmetric crystal structures and the two-photon absorption spectra of complexes of centrosymmetric crystal structures formed from tetraalkylammonium halide and carbon tetrabromide.[20,21]

In this article, we describe systematic quantitative investigations and discuss the intensity-dependent linear absorption and frequency-dependent third-order nonlinear optical properties of the [NR_4Br·CBr_4] (NR_4 = NMe_4, NPr_4, and DBU−H^+) complexes in which the halide salts and carbon tetrabromide are electron-donor/-acceptor dyads. Here, the complex protonated amine bromide/carbon tetrabromide ([DBU−H^+Br^-·CBr_4]) exhibiting strong hydrogen bonds was selected for an investigation of the effect of hydrogen bonds on NLO properties. Details of our computational approach are presented in section 2. In section 3, the results are presented and discussed in relation

† Part of the "Sheng Hsien Lin Festschrift".

* To whom correspondence should be addressed. E-mail: cwd@ms.fjirsm.ac.cn.

10.1021/jp072703+ CCC: $37.00
Published on Web 08/03/2007

to experiments. Finally, we present the conclusions and summarize our findings in section 4.

2. Computational Procedures

Time-dependent density functional theory (TDDFT)[22−24] was employed to compute electronic absorption spectra, and TDDFT combined with the sum-over-states (SOS) method[25,26] was used to calculate the frequency-dependent third-order polarizabilities of different optical processes for the considered complexes. TDDFT based on the B3YLP (TDB3LYP) approximation level was applied to compute electronic excitation energies and using the Gaussian 03 code.[27] The TDDFT method is one of the most popular methods for the calculation of excitation energies in quantum chemistry because of its efficiency and accuracy. It has been used to study the electron spectra and nonlinear optical properties, and the accuracy and reliability of the calculated results have been tested for numerous systems including charge-transfer systems.[15−17,28,29] The standard 6-31+G** basis set was chosen to describe the C, H, and N atoms, and the 3-21G** basis set was used for the halogen atoms. In fact, the convergence behaviors of the basis sets have been tested in calculations of the NLO properties of 2-methyl-4-nitroaniline, and it was found that the second-order polarizabilities obtained using the 3-21G+ and 6-31G+ basis sets were similar in calculations using the ab initio CIS−SOS method.[30] Here, the B3LYP method employs the Becke exchange function combined with three parameters of the Lee−Yang−Parr hybrid correlation functions.[31−33] The wave functions and energy eigenvalues of the excited states were determined by solving the time-dependent Kohn−Sham equation.[34,35] The expression of the third-order polarizability, γ, was obtained by application of time-dependent perturbation theory to the interaction between the electromagnetic field and the microscopic system. Straightforward application of standard quantum mechanical time-dependent perturbation theory, however, leads to unphysical secular divergences in $\gamma_{abcd}(-\omega_p;\omega_1,\omega_2,\omega_3)$ when any subset of the frequencies ω_1, ω_2, and ω_3 sums to zero. Fortunately, the divergences were eliminated by employing the damping factor $i\Gamma$,[3] as described in the equation

$$\gamma_{abcd}(-\omega_p;\omega_1,\omega_2,\omega_3) = (2\pi/h)^3 K(-\omega_p;\omega_1,\omega_2,\omega_3)e^4 \times \left\{ \sum_p \left[\sum_{i,j,k}{}' \frac{\langle o|r_a|k\rangle\langle k|r_b^*|j\rangle\langle j|r_c^*|i\rangle\langle i|r_d|o\rangle}{(\omega_{ko}-\omega_p-i\Gamma_{ko})(\omega_{jo}-\omega_1-\omega_2-i\Gamma_{jo})(\omega_{io}-\omega_1-i\Gamma_{io})} \right] - \sum_p \left[\sum_{j,k}{}' \frac{\langle o|r_a|j\rangle\langle j|r_b|o\rangle\langle o|r_c|k\rangle\langle k|r_d|o\rangle}{(\omega_{jo}-\omega_p-i\Gamma_{jo})(\omega_{jo}-\omega_1-i\Gamma_{jo})(\omega_{ko}+\omega_2+i\Gamma_{ko})} \right] \right\} \quad (1)$$

Here, $\langle o|r_a|k\rangle$ represents an electronic transition moment along the a axis of a Cartesian system, between the reference state $\langle o|$ and the excited state $\langle k|$; $\langle k|r_b^*|j\rangle$ denotes the dipole difference operator, which is equal to $[\langle k|r_b|j\rangle - \langle o|r_b|o\rangle\delta_{kj}]$; and $\hbar\omega_{ko}$ is the energy difference between state k and reference state o. In this study, the transition moments and dipole moments were obtained from the results of TDB3LYP calculations. ω_1, ω_2, and ω_3 are the frequencies of the perturbating radiation fields, and $\omega_p = \omega_1 + \omega_2 + \omega_3$ is the polarization response frequency. The sum over p indicates an average over all permutations of ω_p, ω_1, ω_2, and ω_3 along with the associated indices a, b, c, and d; the sum with the prime symbol indicates a sum over all states except reference state o. The factor $K(-\omega_p;\omega_1,\omega_2,\omega_3)$ accounts for distinguishable permutations of the input frequencies, and its value is given by $2^{-m}D$, where m is the number of nonzero input frequencies minus the number of nonzero output frequencies and D is the number of distinguishable orderings of the set $\{\omega_1, \omega_2, \omega_3\}$. For example, the value of $K(-3\omega;\omega,\omega,\omega) = {}^1/_4$ for third-harmonic generation (THG), $K(-2\omega;0,\omega,\omega) = {}^6/_4$ for electric-field induced second-harmonic generation (EFISHG), and $K(-\omega;\omega,\omega,-\omega) = {}^3/_4$ for degenerate four-wave mixing (DFWM). Accordingly, when the input and output frequencies are all zero, i.e., the static case, $K(0;0,0,0) = 1$ for the THG, EFISHG, and DFWM optical processes. In practical calculations, if ω_1, ω_2, and ω_3 (as well as their arbitrary linear combinations) can be chosen to be far from a resonant frequency, all of the damping factors $i\Gamma$ can be neglected. In this case, although the damping factors are not included in this equation the resonant divergences can be avoided, and the nonresonant third-order polarizability tensor γ can be calculated. Throughout this work, the symbols $\gamma(3\omega)$, $\gamma(2\omega)$, and $\gamma(\omega)$ represent the third-order polarizability of THG $\gamma(-3\omega;\omega,\omega,\omega)$, EFISHG $\gamma(-2\omega;0,\omega,\omega)$, and DFWM $\gamma(-\omega;\omega,\omega,-\omega)$, respectively. The prefactor $K(-\omega_p;\omega_1,\omega_2,-\omega_3)$ is the relative magnitudes of the reference state nonlinear polarizability for each optical process at nonzero frequency. In the following calculations, we used the same prefactor K to justify plotting curves for the nonlinear polarizabilities of the three optical processes against common axes. To obtain a reliable value of γ_{abcd}, accurate values of the transition energies and dipole moments must be used in eq 1. An average $\langle\gamma\rangle$ of the considered species is obtained from the expression

$$\langle\gamma\rangle = {}^1/_5(\gamma_{xxxx} + \gamma_{yyyy} + \gamma_{zzzz} + \gamma_{xxyy} + \gamma_{xxzz} + \gamma_{yyxx} + \gamma_{yyzz} + \gamma_{zzxx} + \gamma_{zzyy}) \quad (2)$$

Calculations of γ are concerned only with contributions from electric dipole transitions because they are much more intense than vibrational and rotational transitions.[36] In the following discussions, we provide systematic comparisons of only the third-order nonlinear optical properties among the studied species and omit vibrational and rotational contributions to polarizabilities or hyperpolarizabilities. Electron−electron interactions (EEIs) or configuration interactions are included in a natural way in the TDDFT calculations.[37] Accordingly, a time-dependent DFT formalism was employed to compute excitation-energy and frequency-dependent response functions of γ, and it rectified the EEI problems of the ab initio SCF approximation at comparable or even lower computational cost.[23] The self-consistent field (SCF) convergence criteria were set by the default values of the Gaussian 03 program in the excited-state calculations. The core orbitals were frozen in the correlation calculations. The iterations of excited states were continued until the changes in the energies of the states were no more than 10^{-7} a.u. between the iterations, and convergence was reached in all calculations of excited states. In the calculation of γ, we used only about 50 excited states in the summations of the SOS expansion, and convergence of γ was reached well.

3. Results and Discussion

A. Geometries and Electronic Structures in the Ground State. Configurations of the considered complexes of carbon tetrabromide tetraalkylammonium halide are shown in Figure 1. Two series of donor−acceptor dyads were formed in these molecules. In the first, carbon tetrabromide served as the electron acceptor, and tetraethylammonium halide served as the electron donor with the halide as chloride, bromide, and iodide. In the second, the counterion was of progressively growing size (alkyl = Me, Et, Pr, and DBU−H$^+$). Such D−A structures are typically associated with the charge-transfer character of

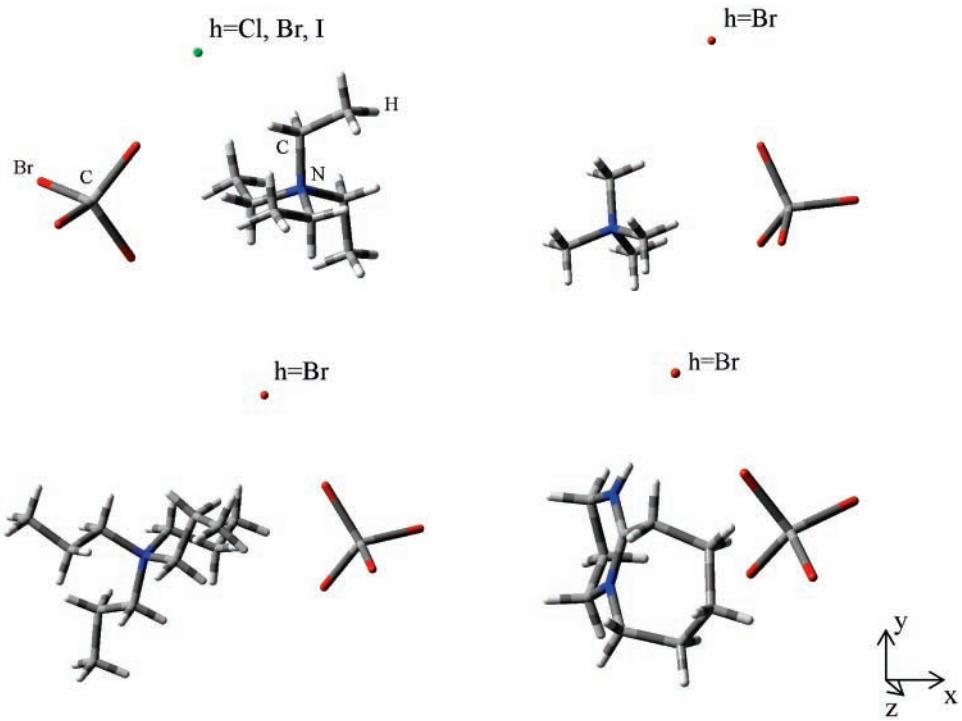

Figure 1. Geometric structures of the investigated electron-donating−electron-accepting tetraalkylammonium halide/carbon tetrabromide complexes [NR_4h·CBr_4] (h = Cl, Br, and I; NR_4 = NMe_4, NEt_4, NPr_4, and DBU−H^+).

TABLE 1: Selected Donor−Acceptor Distances and C−Br···*h* Angles for the Considered Complexes

compound	$R_{h\cdots BrCBr_3}$ (Å)	$A_{C-Br\cdots h}$ (deg)	compound	$R_{Br\cdots BrCBr_3}$ (Å)	$A_{C-Br\cdots h}$ (deg)
NEt_4Cl·CBr_4	3.090	174.987	NMe_4Br·CBr_4	3.332	180.0
NEt_4Br·CBr_4	3.154	175.218	NPr_4Br·CBr_4	3.187	177.087
NEt_4I·CBr_4	3.298	176.522	DBU−H^+Br^-·CBr_4	3.260	175.774

intermolecular [Br_3CBr···halide] interactions. In Table 1, we list the characteristic distances between the donor and the acceptor and the angles of the C−Br(CBr_4)···h(donor) in the charge-transfer direction to investigate the effects of structure on optical properties. It is shown that the separation between the donor and acceptor increases from 3.090 to 3.298 Å when the halogen donor strengthens from chloride to iodide for the [NEt_4h·CBr_4] (h = Cl, Br, and I) series and from 3.154 to 3.260 Å when the counterion changes from Et to Pr to DBU−H^+, except for R_4 = Me_4 which has a length of 3.332 Å for the [NR_4Br·CBr_4] complex. The C−Br···h angles range from 174° to 180° for the considered compounds, which is in the charge-transfer direction between the donor and acceptor.

B. Linear Absorption. In this study, we mainly focus on the effect of the counterion on the optical properties. Figure 2 shows plots of the calculated absorption spectra of [NR_4Br·CBr_4] (NR_4 = NMe_4, NEt_4, NPr_4, and DBU−H^+). To make a comparison, we also provide the calculated absorption spectra of [NEt_4h·CBr_4] (h = Cl, Br, I). It can be seen that the series of considered complexes exhibit electronic transitions in the visible range from 500 to 700 nm (Q band) and in the near-UV range at about 270 nm (B band). The first and second optically allowed excited states with detailed values of transition dipole moments and excitation energies are listed in Table 2. Here, it is noted that the first allowed transition energies calculated at the TDDFT/6-31+G** (/3-21G** for halogen atoms) level in this work are smaller than those calculated at the TDDFT/3-21G* level in our earlier study[20] by about 10% to 4% from Cl to I for [NEt_4h·CBr_4] complexes, although the trends in both are the same. For the [NR_4Br·CBr_4] (NR_4 = NMe_4, NPr_4, and DBU−H^+) complexes consisting in centrosymmetric crystal structures, the absorption peaks undergo a slight blue shift from 689.0 to 597.7 to 538.4 nm in the low-energy region and from 274.1 to 272.7 to 265.5 nm in the high-energy region in order from Me_4 to Pr_4 to DBU−H^+. For the [NEt_4h·CBr_4] (h = Cl, Br, and I) complexes of noncentrosymmetric crystal structures, the absorption peaks show a red shift from 522.8 to 537.3 to 556.6 nm in the low-energy region (Q band) and from 265.9 to 273.9 to 282.8 nm in the high-energy region (B band) as the donor strength increases from Cl to Br to I.

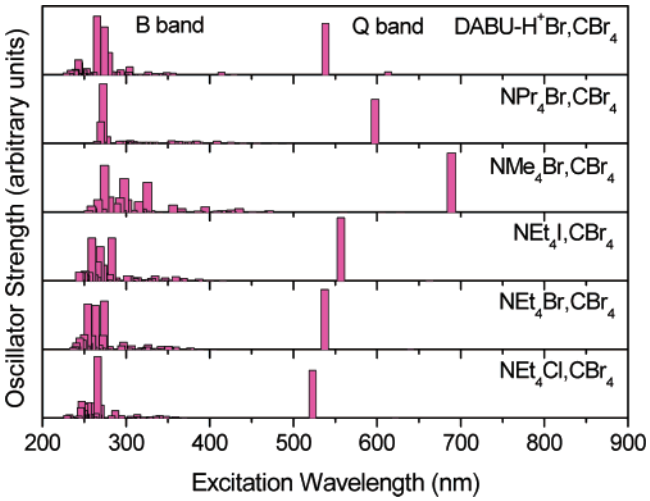

Figure 2. Calculated absorption spectra of [NR_4h·CBr_4] (h = Cl, Br, and I for R = Et and NR_4 = NMe_4, NEt_4, NPr_4, and DBU−H^+ for h = Br) at the TDB3LYP/6-31+G** level.

In the following discussion, we analyze the nature of the excited states contributing to the linear absorption with the orbital distribution. For all of the studied complexes, the first

TABLE 2: Linear Absorption Properties of Compounds

molecule	E_{ge}^{OPA} [a] (eV)	moment (a.u.) x	Y	Z	$E_{ge'}^{OPA}$ [a] (eV)	moment (a.u.) x	Y	Z
NEt_4Cl, CBr_4	2.371	0.892	1.100	−0.130	4.663	−0.680	−0.927	0.088
NEt_4Br, CBr_4	2.308	1.035	1.111	−0.082	4.527	−0.647	−0.729	0.046
NEt_4I, CBr_4	2.228	1.247	1.143	−0.059	4.385	−0.721	−0.684	0.014
NMe_4Br, CBr_4	1.800	1.088	−1.321	0.006	4.523	0.450	−0.847	0.031
NPr_4Br, CBr_4	2.074	0.588	1.410	0.253	4.546	−0.416	−1.134	−0.134
DBU−H^+Br^-, CBr_4	2.303	0.976	1.011	−0.125	4.671	0.662	0.814	−0.129

[a] E_{ge}^{OPA} and $E_{ge'}^{OPA}$ are the calculated vertical excitation energies of the first (e) and second (e′) optically allowed excited states with the corresponding transition dipole moments.

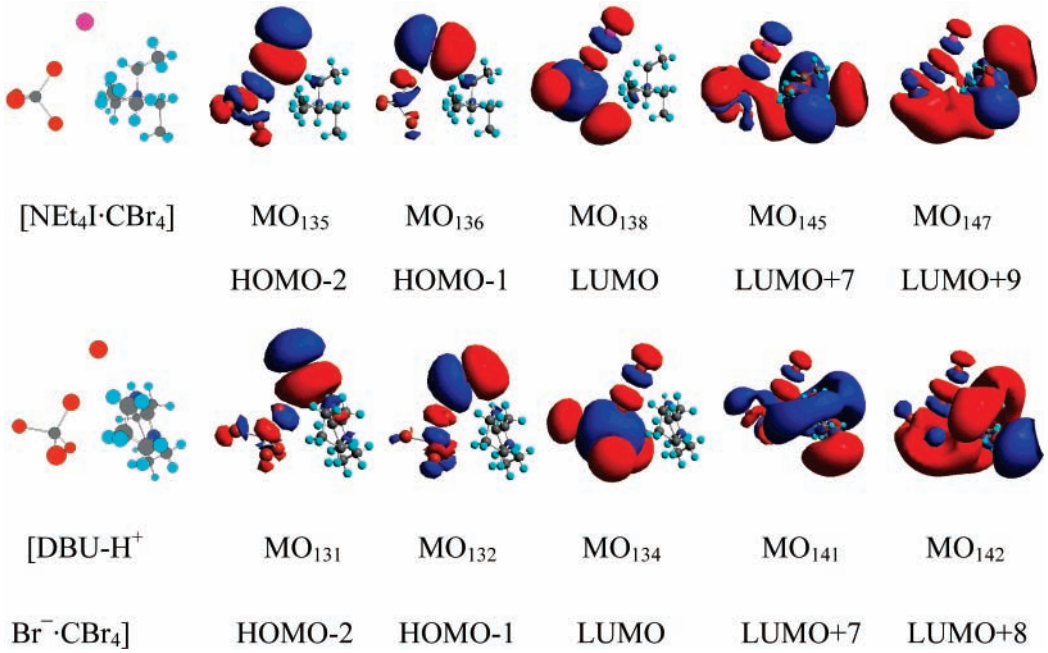

Figure 3. Orbital configurations of [NEt_4I·CBr_4] and [DBU−H^+ Br^-·CBr_4].

allowed excited state mostly originates from an electronic transition from the ground singlet state to excited singlet state S_3, and the second allowed excited state is mostly derived from an electronic transition from the ground singlet state to excited singlet state S_n, where $n = 29$ for the [NEt_4h·CBr_4] (h = Cl, Br, and I), $n = 45$ for [NMe_4Br·CBr_4], $n = 46$ for [NPr_4Br·CBr_4], and $n = 30$ for [DBU−H^+Br^-·CBr_4]. From analysis of the configuration state combined with molecular orbital components, we found that the absorption peaks in the Q band contributed from the S_3 state mainly arise from charge transfers from the halogen ion to carbon tetrabromide, whereas the absorption peaks in the B band contributed from the S_n state can be described as contributions of charge transfers from halogen ion orbitals to the mixing orbitals of carbon tetrabromide and the counterion. For example, excited state S_3 consists of contributions from the configurations 0.62055(MO_{135} → MO_{138}) and 0.16483(MO_{136} → MO_{138}), and excited state S_{29} consists chiefly of contributions from the configurations 0.61037(MO_{135} → MO_{145}) and 0.14834(MO_{135} → MO_{147}) for [NEt_4I·CBr_4]. We show plots of these relevant transition orbitals for the selected compounds in Figure 3. In this figure, it can be seen that HOMO − 1 (MO_{135}) and HOMO − 2 (MO_{136}) are mostly made up of contributions from halogen atomic orbitals; however, the LUMO (MO_{138}) consists mostly of contributions from the group orbitals of carbon tetrabromide, and LUMO + 7 (MO_{145}) and LUMO + 9 (MO_{147}) are made up of contributions from the mixing orbitals of carbon tetrabromide and the counterion. Similarly, the molecular orbital plots of [DBU−H^+ Br^-·CBr_4] also provide evidence for the assignments of the Q and B absorption bands. Overall, the calculations accurately reproduce the bathochromic shifts of the absorption maxima with increased donor strength observed in the experimental measurements.[19]

C. Third-Order Nonlinear Optical Response. Here, we consider only the complexes of carbon tetrabromide and tetraalkylammonium halide with centrosymmetric crystal structures, i.e., [NR_4Br·CBr_4] (NR_4 = NMe_4, NPr_4, and DBU−H^+), in the calculations of third-order polarizabilities. The transition energies from the ground state to excited states, the electronic dipole moments of the ground state and excited states, and the transition moments from the ground or excited state to excited states were calculated by the TDB3LYP method. The obtained values were taken as input for the SOS equation. Before attempting to compute the variation of the third-order polarizability vs frequency, it was necessary to investigate the behavior of the convergence in the summation of the excited states and to determine whether the results calculated by the TDB3LYP method are reliable for [NR_4Br·CBr_4]. As for the calculation of γ, we generally truncated the infinite SOS expansion to a finite expression after apparent convergence of γ had been reached. Figure 4 shows plots of the calculated third-order polarizability γ_{yyyy} component against the number of states in the nonresonant region of input energies of 0.0, 0.55, and 0.80

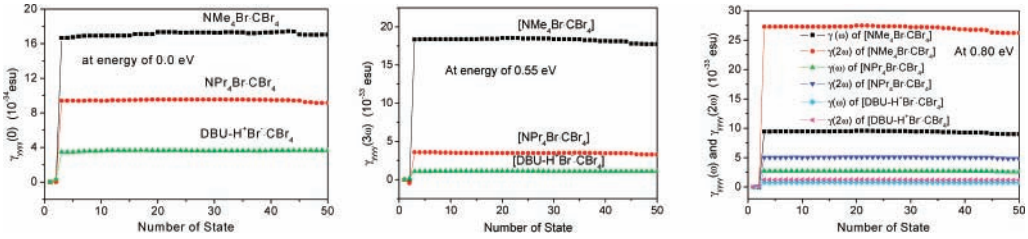

Figure 4. Convergence behavior of γ with the number of states considered in the calculations by the SOS//TDB3LYP/6-31+G** method at different input energies.

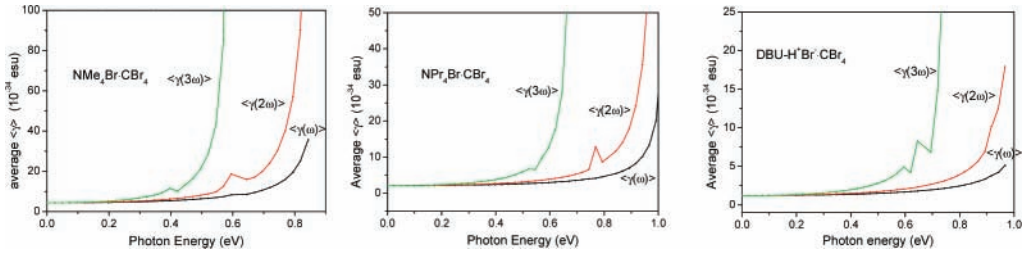

Figure 5. Dynamic third-order optical polarizabilities of three optical processes in the low-frequency region as calculated by the SOS//TDB3LYP/6-31+G** method.

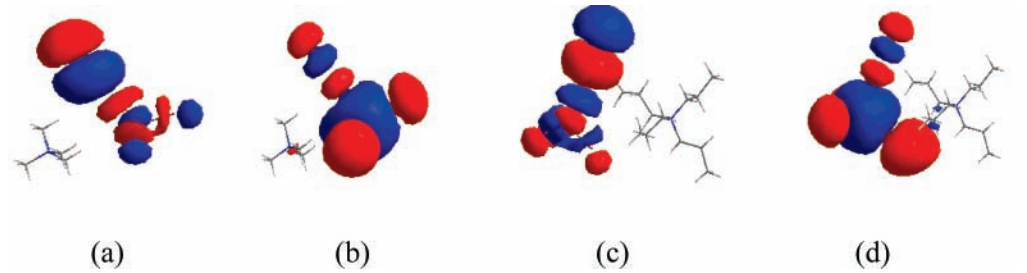

Figure 6. Surface plots of (a) HOMO − 2 (MO_{110}) and (b) LUMO (MO_{113}) for [NMe_4Br·CBr_4] and of (c) HOMO − 2 (MO_{142}) and (d) LUMO (MO_{145}) for [NPr_4Br·CBr_4].

eV in the three optical processes. Our calculated results show that the third-order polarizability along the *y* direction (see Figure 1) of both incident and polarization light makes the largest contribution to the average third-order polarizability of $\langle\gamma\rangle$. It can be seen in Figure 4 that the curves have very similar convergence behaviors and the third excited state makes a very significant contribution to the third-order polarizability. The calculated values of γ_{yyyy} including three states are not less than 90% of the values obtained by including 50 states for all. This indicates that a reasonable approximation can be obtained by truncating the infinite SOS expansion to a finite sum over 50 states in our calculations of γ.

Now, we discuss the third-order optical properties based on the calculated results at the ground state. The average $\langle\gamma\rangle$ value with different counterions can be obtained from eq 2. Figure 5 depicts the dynamic $\langle\gamma\rangle$ values of the three optical physical process (THG, EFISHG, and DFWM) for [NR_4Br·CBr_4] (NR_4 = NMe_4, NPr_4, DBU−H^+) as the input photon energy increases from 0.0 to 1.0 eV. It shows that the preresonant frequency of the third-order polarizability decreases as the number of frequencies at the optical polarization increases. For example, the preresonant frequencies of $\langle\gamma(\omega)\rangle$, $\langle\gamma(2\omega)\rangle$, and $\langle\gamma(3\omega)\rangle$ are at 0.818, 0.719, and 0.521 eV/$\hbar$, respectively, for the [NMe_4-Br·CBr_4] complex. In the static case where the input energy is zero, the third-order polarizability of $\langle\gamma(0)\rangle$ decreases in the order [NMe_4Br·CBr_4] (4.344×10^{-34} esu) > [NPr_4Br·CBr_4] (2.087×10^{-34} esu) > [DBU−H^+Br^-·CBr_4] (1.200×10^{-34} esu). In dynamic cases where the input frequency is in the nonresonant region, the third-order polarizabilities of $\langle\gamma(\omega)\rangle$, $\langle\gamma(2\omega)\rangle$, and $\langle\gamma(3\omega)\rangle$ decrease in the same order as in the static case for the [NR_4Br·CBr_4] complexes. For instance, $\langle\gamma(\omega)\rangle$, $\langle\gamma(2\omega)\rangle$, and $\langle\gamma(3\omega)\rangle$ at the input energy of 0.546 eV are 7.014×10^{-34}, 9.800×10^{-34}, and 43.883×10^{-34} esu, respectively, for [NMe_4Br·CBr_4]; 2.769×10^{-34}, 3.406×10^{-34}, and 6.576×10^{-34} esu, respectively, for [NPr_4Br·CBr_4]; and 1.577×10^{-34}, 1.858×10^{-34}, and 3.516×10^{-34} esu, respectively, for [DBU−H^+Br^-·CBr_4]. The nonresonant frequency region of the [NMe_4Br·CBr_4] complex is narrow, although it has larger polarizabitities compared to other complexes.

The electronic origin of the third-order polarizability is discussed for the [NR_4Br·CBr_4] complexes in this section. From the plots in Figure 4 of the state-dependent third-order polarizabilities, one can see that the third-order polarizabilities of the [NR_4Br·CBr_4] complexes are mostly made up of contributions from the third excited state S_3. The largest components of the S_3 state are from the configurations $0.5987(\psi_{110\rightarrow113})$, $0.6312(\psi_{142\rightarrow145})$, and $0.5278(\psi_{131\rightarrow134})$ for the [NR_4Br·CBr_4] complexes with NR_4 = NMe_4, NPr_4, and DBU−H^+, respectively. These configuration states are all constructed by promotion of one electron from HOMO − 2 to the LUMO. The electronic structure calculations show that HOMO − 2 receives the most contributions from orbitals of the Br donor and the LUMO has significant contributions from the acceptor [CBr_4] group orbitals. The molecular orbital plots in Figures 6 and 3 provide this evidence. At the end, we conclude that the donor−acceptor charge transfers, i.e., electronic transitions from HOMO − 2 to the LUMO, make a direct contribution to the third-order polarizability for the [NR_4Br·CBr_4] (NR_4 = NMe_4, NPr_4, and DBU−H^+) complexes. However, to determine the role of the counterions in the third-order optical response on these com-

plexes, we made detailed analyses of the donor−acceptor interactions through the bond lengths listed in Table 1. It is found that there is a weaker interaction between the donor and acceptor for the small counterion Me than for the large counterion Pr. The weak interaction between the donor and acceptor chromophores results in a red shift of the electronicabsorption band (i.e., reduction of the electron transition energy), further leading to the larger third-order polarizability of the [$NMe_4Br{\cdot}CBr_4$] complex. The [$DBU{-}H^+Br^-{\cdot}CBr_4$] complex contains strong $N^+H\cdots Br^-$ hydrogen bonds in its structure, although it has a weaker interaction (greater distance) between the donor and acceptor than does the [$NPr_4Br{\cdot}CBr_4$] complex. This is the reason why the third-order polarizability of the [$DBU{-}H^+Br^-{\cdot}CBr_4$] complex with the weaker interaction between the donor and acceptor is larger than that of [$NPr_4Br{\cdot}CBr_4$]. From such analyses, we believe that the counterions in these complexes indirectly affect the third-order polarizability through their influences on the donor−acceptor interactions.

4. Conclusion

Linear and nonlinear optical properties for a series of donor−acceptor chromophores such as tetraalkylammonium halide/carbon tetrabromide, [$NR_4h{\cdot}CBr_4$] (h = Cl, Br, and I; NR_4= NMe_4, NEt_4, NPr_4, and $DBU{-}H^+$) have been calculated in view of the structure/property relationships using the TDDFT technique combined with the SOS method, showing that the investigated electron-donating−electron-accepting complexes exhibit large third-order polarizabilities. The charge-transfer nature of the $Br_3CBr\cdots$halide association represents a dominant factor in the third-order polarizability, and the counterion indirectly affects the electronic absorption and third-order polarizability spectra through the interactions between the donor and acceptor. Our results show that the third-order polarizability increases in the order [$DBU{-}H^+Br^-{\cdot}CBr_4$] < [$NPr_4Br{\cdot}CBr_4$] < [$NMe_4Br{\cdot}CBr_4$] and the absorption peaks show a red shift as the donor strength increases from Cl to Br to I for the [$NEt_4h{\cdot}CBr_4$] (h = Cl, Br, and I) complexes.

Acknowledgment. The authors are grateful to the National Science Foundation of China (No. 20373073), the National Basic Research Program of China (No. 2004CB720605), the Funds of the Chinese Academy of Sciences and Fujian Key Laboratory of Nanomaterials (KJCX2-YW-H01 and No. 2006L2005), and the Foundation of the State Key Laboratory of Structural Chemistry (030060) for financial support.

References and Notes

(1) de Jong, J. J. D.; Lucas, L. N.; Kellogg, R. M.; van Esch, J. H.; Feringa, B. L. *Science* **2004**, *304*, 278−281.
(2) Mustroph, H.; Stollenwerk, M.; Bressau, V. *Angew. Chem., Int. Ed.* **2006**, *45*, 2016−2035.
(3) Bredas, J. L.; Adant, C.; Tackx, P.; Persoons, A.; Pierce, B. M. *Chem. Rev.* **1994**, *94*, 243.
(4) Li, Q. S.; Liu, C. L.; Liu, Z. G.; Gong, Q. H. *Opt. Express* **2005**, *13*, 1833.
(5) Karna, S. P.; Yeates, A. T. *Nonlinear Optical Materials*; American Chemical Society: Washington, DC, 1996.
(6) Spassova, M.; Enchev, V. *Chem. Phys.* **2004**, *298*, 29.
(7) Bhawalkar, J. D.; He, G. S.; Prasad, P. N. *Rep. Prog. Phys.* **1996**, *59*, 1041.
(8) Matsuzaki, Y.; Nogami, A.; Tsuda, A.; Osuka, A.; Tanaka, K. *J. Phys. Chem. A* **2006**, *110*, 4888−4899.
(9) Zheng, W. X.; Wong, N. B.; Li, W. K.; Tian, A. M. *J. Chem. Theory Comput.* **2006**, *2*, 808−814.
(10) Collini, E.; Ferrante, C.; Bozio, R.; Lodi, A.; Ponterini, G. *J. Mater. Chem.* **2006**, *16*, 1573−1578.
(11) Qin, J. G.; Liu, D. Y.; Dai, C. Y. *Coord. Chem. Rev.* **1999**, *188*, 23.
(12) Han, H. Y.; Song, Y. L.; Hou, H. W.; Fan, Y. T.; Zhu, Y. *Dalton Trans.* **2006**, 1972−1980.
(13) Kuzyk, M. G. *Phys. Rev. Lett.* **2000**, *85*, 1218.
(14) Rumi, M.; Ehrlich, J. E.; Heikal, A. A.; Perry, J. W.; Barlow, S.; Hu, Z. Y.; McCord-Maughon, D.; Parker, T. C.; Rockel, H.; Thayumanavan, S.; Marder, S. R.; Beljonne, D.; Bredas, J. L. *J. Am. Chem. Soc.* **2000**, *122*, 9500.
(15) Day, P. N.; Nguyen, K. A.; Pachter, R. *J. Phys. Chem. B* **2005**, *109*, 1803−1814.
(16) Badaeva, E. A.; Timofeeva, T. V.; Masunov, A.; Tretiak, S. *J. Phys. Chem. A* **2005**, *109*, 7276−7284.
(17) Kwon, O.; Barlow, S.; Odom, S. A.; Beverina, L.; Thompson, N. J.; Zojer, E.; Bredas, J. L.; Marder, S. R. *J. Phys. Chem. A* **2005**, *109*, 9346−9352.
(18) Creighton, J. A.; Thomas, K. M. *J. Chem. Soc., Dalton Trans.* **1972**, 403.
(19) Lindeman, S. V.; Hecht, J.; Kochi, J. K. *J. Am. Chem. Soc.* **2003**, *125*, 11597.
(20) Cheng, W.-D.; Shen, J.; Wu, D.-S.; Li, X.-D.; Lan, Y.-Z.; Li, F.-F.; Huang, S.-P.; Zhang, H.; Gong, Y.-J. *Chem. Eur. J.* **2006**, *12*, 6880−6887.
(21) Shen, J.; Cheng, W.-D.; Wu, D.-S.; Lan, Y.-Z.; Li, F.-F.; Huang, S.-P.; Zhang, H.; Gong, Y.-J. *J. Phys. Chem. A* **2006**, *110*, 10330−10335.
(22) Stratmann, R. E.; Scuseria, G. E.; Frisch, M. J. *J. Chem. Phys.* **1998**, *109*, 8218.
(23) Bauemschmitt, R.; Ahlrichs, R. *Chem. Phys. Lett.* **1996**, *256*, 454.
(24) Casida, M. E.; Jamorski, C.; Casida, K. C.; Salahub, D. R. *J. Chem. Phys.* **1998**, *108*, 4439.
(25) Orr, B. J.; Ward, J. F. *Mol. Phys.* **1971**, *20*, 513.
(26) Pierce, B. M. *J. Chem. Phys.* **1989**, *91*, 791.
(27) Frisch, M. J.; Trucks, G. W.; Schlegel, H. B.; Scuseria, G. E.; Robb, M. A.; Cheeseman, J. R.; Montgomery, J. A., Jr.; Vreven, T.; Kudin, K. N.; Burant, J. C.; Millam, J. M.; Iyengar, S. S.; Tomasi, J.; Barone, V.; Mennucci, B.; Cossi, M.; Scalmani, G.; Rega, N.; Petersson, G. A.; Nakatsuji, H.; Hada, M.; Ehara, M.; Toyota, K.; Fukuda, R.; Hasegawa, J.; Ishida, M.; Nakajima, T.; Honda, Y.; Kitao, O.; Nakai, H.; Klene, M.; Li, X.; Knox, J. E.; Hratchian, H. P.; Cross, J. B.; Bakken, V.; Adamo, C.; Jaramillo, J.; Gomperts, R.; Stratmann, R. E.; Yazyev, O.; Austin, A. J.; Cammi, R.; Pomelli, C.; Ochterski, J. W.; Ayala, P. Y.; Morokuma, K.; Voth, G. A.; Salvador, P.; Dannenberg, J. J.; Zakrzewski, V. G.; Dapprich, S.; Daniels, A. D.; Strain, M. C.; Farkas, O.; Malick, D. K.; Rabuck, A. D.; Raghavachari, K.; Foresman, J. B.; Ortiz, J. V.; Cui, Q.; Baboul, A. G.; Clifford, S.; Cioslowski, J.; Stefanov, B. B.; Liu, G.; Liashenko, A.; Piskorz, P.; Komaromi, I.; Martin, R. L.; Fox, D. J.; Keith, T.; Al-Laham, M. A.; Peng, C. Y.; Nanayakkara, A.; Challacombe, M.; Gill, P. M. W.; Johnson, B.; Chen, W.; Wong, M. W.; Gonzalez, C.; Pople, J. A. *Gaussian 03*, revision C.02; Gaussian, Inc.: Pittsburgh, PA, 2004.
(28) (a) De Angelis, F.; Fantacci, S.; Sgamelotti, A.; Cariati, F.; Roberto, D.; Tessore, F.; Ugo, R. *Dalton Trans.* **2006**, 852−859. (b) Coe, B. J.; Beljonne, D.; Vogel, H.; Garin, J.; Orduna, J. *J. Phys. Chem. A* **2005**, *109*, 10052−10057.
(29) Bartholomew, G. P.; Rumi, M.; Pond, S. J. K.; Perry, J. W.; Tretiak, S.; Bazan, G. C. *J. Am. Chem. Soc.* **2004**, *126*, 11529−11542.
(30) Cheng, W.-D.; Wu, D.-S.; Zhang, H.; Li, X.-D.; Chen, D.-G.; Lang, Y.-Z.; Zhang, Y.-C.; Gong, Y.-J. *J. Phys. Chem. B* **2004**, *108*, 12658−12664.
(31) Becke, A. D. *J. Chem. Phys.* **1993**, *98*, 5648.
(32) Lee, C.; Yang, W.; Parr, R. G. *Phys. Rev. B* **1988**, *37*, 785.
(33) Miehlich, B.; Savin, A.; Stoll, H.; Preuss, H. *Chem. Phys. Lett.* **2000**, *157*, 1989.
(34) Gross, E. K. U.; Kohn, W. *Adv. Quantum Chem.* **1990**, *21*, 255.
(35) Runge, E.; Gross, E. K. U. *Phys. Rev. Lett.* **1984**, *52*, 997.
(36) Atkins, P. W. *Molecular Quantum Mechanics*, 2nd ed.; Oxford University Press: New York, 1983; Chapter 11.
(37) van Gisbergen, S. J. A.; Snijders, J. G.; Baerends, E. J. *Comput. Phys. Commun.* **1999**, *118*, 119.